PNAS RESEARCH ARTICLE | EVOLUTION

Genetic, phenotypic, and environmental drivers of local adaptation and climate change–induced maladaptation in a migratory songbird

Marina D. Rodriguez[a,1], Christen M. Bossu[a], Eric C. Anderson[a], Rachael A. Bay[b], and Kristen C. Ruegg[a]

Edited by Marcus Feldman, Stanford University, Stanford, CA; received July 14, 2025; accepted August 12, 2025

Understanding processes driving local adaptation in wild species is a key goal in evolutionary biology, but linking genotype to phenotype to environmental drivers of natural selection remains challenging. Even more rare are empirical examples of what happens when genotype and phenotype fail to keep pace with environmental change. Here, we explore these connections by conducting an integrative study on the breeding range of the yellow warbler (*Setophaga petechia*). Using genome-wide association studies (GWAS), we first identify loci associated with variation in bill morphology and individual quality. We then employ gene–environment association (GEA) analyses and find that precipitation is a key environmental driver of putative selection on bill shape. Finally, we test whether contemporary individuals whose bill shapes deviate from the historical relationship with precipitation experience increased stress (measured by telomere length) as a result of maladaptation. We also use historical DNA to test whether local populations have shifted their ranges over the past century, confirming that the observed changes are not due to range shifts. Our results align with predictions from GWAS and GEA analyses, indicating that birds with shallower bills in increasingly arid regions suffer higher stress (i.e., shorter telomeres) because of maladaptation. Overall, this study links genetic, phenotypic, and environmental data with stress biomarkers to improve understanding of the process of local adaptation and the consequence of failing to keep pace with changing climate conditions.

local adaptation | genome-wide association study (GWAS) | gene–environment analysis (GEA) | telomere length | bill morphology

Significance

As climate change alters environments, many wild populations are struggling to keep up. However, empirical examples of what happens when genotype and phenotype fail to track environmental change remain rare. Here, we identify genetic and environmental factors shaping bill morphology in a migratory bird and show that birds whose bills are failing to keep pace with changes in local climate are exhibiting greater physiological stress. By integrating historical DNA, genome-wide data, morphology, and telomere length as a biomarker of stress, this work provides rare empirical evidence of contemporary maladaptation in the wild. These findings highlight the importance of linking genes, traits, and environment to understand species' responses to rapid climate change.

Local adaptation occurs when populations evolve in response to divergent selection across heterogeneous environments (1). While identifying local adaptation in wild populations remains a central goal of evolutionary biology, clear examples where both the genetic basis of a key phenotype and the environmental drivers of natural selection are well understood are still relatively rare (but see refs. 2–4). Many of the best-characterized examples of local adaptation involve traits with simple genetic architectures, where a single or few loci drive major phenotypic changes in response to selection. However, as more complex traits come under investigation, our understanding of the genetic basis of local adaptation is expanding. A compelling case of this progress can be found in Darwin's finches, where beak size of the medium ground finch is known to increase in response to drought-induced decreases in the availability of smaller, softer seeds (5). Although the genetic basis of beak morphology in Darwin's finches is complex, key genes such as *HMGA2* and *ALX1* have been linked to beak size and shape and may allow for rapid evolutionary responses to shifts in precipitation (5, 6). As climate change continues to drive fluctuations in temperature and precipitation, understanding both simple and complex genetic architectures underlying local adaptation is becoming increasingly important for predicting how species may respond to global change.

In the era of Next-Generation Sequencing, genome-wide association studies (GWAS) have become a powerful approach for uncovering the genetic basis of traits linked to fitness and local adaptation (7). A GWAS uses linear mixed models to find significant associations between loci associated with specific phenotypes across a large sample of individuals (8). This approach has been useful for identifying key genes underlying traits important to fitness across a variety of taxa, including autoimmune diseases in humans (9), reproductive behavior in steelhead trout (*Oncorhynchus mykiss*) (10), and the genetic architecture of migratory direction in mule deer (*Odocoileus hemionus*) (11). In birds, bill shape is a good candidate phenotype for a GWAS because it often varies between populations, is highly heritable, and has established links to individual fitness across species (12, 13). Further, numerous studies have connected bill morphology to climate, showing that larger bills are an adaptation to hot, dry conditions (14–16). After identifying genotype–phenotype links through a GWAS, a comprehensive understanding of the role of bill morphology in

Author affiliations: [a]Department of Biology, Colorado State University, Fort Collins, CO 80523; and [b]Department of Evolution and Ecology, University of California, Davis, CA 95616

Author contributions: M.D.R. and K.C.R. designed research; M.D.R. performed research; M.D.R. contributed new reagents/analytic tools; M.D.R., C.M.B., E.C.A., and R.A.B. analyzed data; and M.D.R. and K.C.R. wrote the paper.

The authors declare no competing interest.

This article is a PNAS Direct Submission.

PNAS policy is to publish maps as provided by the authors.

[1]To whom correspondence may be addressed. Email: mdrodriguez10@gmail.com.

This article contains supporting information online at https://www.pnas.org/lookup/suppl/doi:10.1073/pnas.2518497122/-/DCSupplemental.

Published September 29, 2025.

local adaptation necessitates examination of the environmental variables underlying natural selection.

Gene–environment association (GEA) methods are phenotype-free approaches that combine landscape and population genomics to identify environmental variables shaping adaptive genetic variation (17). For instance, recent studies have used GEA-based approaches to detect genomic signals of local adaptation to urban habitats in the bird species, *Parus major*, across Europe (18) and to snowpack in willow leaf beetles (*Chrysomela vigintipunctata*) (19). In GEAs, the emphasis is put on selecting climate variables that may capture the drivers of selection at the correct spatial and temporal scale. Although both GWAS and GEA are commonly employed in studies of local adaptation, using them independently can limit their scope. Alternatively, combining these approaches allows researchers to gain a more comprehensive understanding of the genetic basis of traits important to local adaptation, and the environmental factors driving selection (e.g., refs. 20 and 21).

Perhaps the most critical and difficult step with identifying the genetic basis of traits important to local adaptation is validating the role of candidate genes in fitness and/or individual quality. Measuring individual quality is challenging in many species because it often requires monitoring offspring across multiple generations. Measuring telomere length, however, provides a promising and cost-effective alternative for assessing individual quality in species where offspring tracking is unfeasible. Telomeres are noncoding, specialized DNA sequences at the ends of chromosomes that maintain chromosome stability and protect coding DNA from erosion (22). Prior research has demonstrated that stressful environments can accelerate telomere attrition (23, 24) and faster rates of telomere shortening can predict mortality (25, 26). Telomere length is also known to vary with individual quality (i.e., refs. 27 and 28) and fitness across a variety of taxa (e.g., refs. 25, 29, and 30). Comparative measures of telomere length between individuals can be used to test hypotheses about phenotypic traits important to local adaptation in species where field-intensive assessments of individual quality are impractical.

The yellow warbler (*Setophaga petechia*), a migratory songbird with a breeding distribution that extends across North America, is a good system in which to identify the links between genotype, phenotype, and the environment, because extensive prior research on all three aspects provides a strong foundation for generating testable hypotheses. Past work has shown a positive correlation between bill depth and precipitation prior to 1950 (31), offering a historical baseline from which to assess how deviations from this preclimate change relationship may impact individual quality. Previous GEA analyses further suggest that precipitation is the primary driver of genetic variation across space and that recent population declines are linked to climate change–induced shifts in precipitation (32, 33). Collectively, these findings support the hypothesis that bill shape is critical to local adaptation in yellow warblers and that changes in precipitation may drive selection on this trait. Consequently, we predict that a failure to adjust bill shape in response to shifts in precipitation will lead to reduced individual quality and population declines.

To identify the links between genotype, phenotype, and environmental drivers of natural selection in the yellow warbler, and to test how climate change–induced mismatches may lead to maladaptation, we integrate measurements of bill shape (from both past and present) with a GWAS, GEA, and telomere length assessments across populations. We first conduct a GWAS in two populations to identify the genetic basis of bill shape and intersect these genes with a GWAS on telomere length (Fig. 1*A*) to focus on genes important to individual quality (Fig. 1*B*). To test whether bill size mediates local adaptation to precipitation regimes, we then conduct a GEA on bill-linked loci identified through GWAS to determine the environmental drivers of variation in these subsets of putatively adaptive loci for 22 populations across the breeding range (Fig. 1*C*). To investigate whether maladaptation may contribute to recent population declines, we examine how deviations from the preclimate change baseline relationship between bill shape and precipitation impact individual quality, as measured by telomere length (Fig. 1 *E*–*H*). If recent population declines result from a failure to adjust bill size in response to changes in precipitation, we predict that populations exhibiting the greatest deviation from the preclimate change relationship will experience the highest levels of stress and, consequently, have the shortest telomeres. Additionally, to rule out the possibility that contemporary patterns may have been influenced by large-scale range shifts rather than maladaptation, we compare genetic structure between historical and contemporary samples across the breeding range. Overall, our results enhance our understanding of the connections between phenotype, genotype, and the environmental drivers of natural selection, which are crucial for assessing the potential threats posed by global environmental change on this species and others.

Results

GWAS Analysis of Telomere Length and Bill Depth Phenotypes. In the bill depth GWAS, a median of 66% of phenotypic variation was explained by the genotype (95% CI 0.08 to 0.99), of which 45% was explained by SNPs with nonzero effects, but the credible intervals on both estimates were very high (95% CI 0.005 to 0.94). Approximately 40% of the variants had nonzero effects (n = 1,069,830); however, 67 were considered to have major effects. We defined the top candidate SNPs as those that were found with sparse effects in at least 1% of the Markov Chain Monte Carlo (MCMC) runs of a single chain (PIP > 0.01), after controlling for population structure (Fig. 2*A*). We identified five candidate SNPs, with the strongest statistical association observed for a SNP on chromosome 4, located within the intronic region of the *CCDC109B* gene (Table 1). One of the remaining four top candidate SNPs was found on chromosome 13 located within the intronic region of *GABRB2*, while the remaining three were found on chromosomes 2 and 18, within the intronic and regulatory regions of uncharacterized proteins. Of the 5 top candidate SNPs, only one overlapped with nonzero effect loci identified in the telomere GWAS, within the *CCDC109B* gene (Table 1).

In the telomere length GWAS, a median of 68% of phenotypic variation was explained by the genotype (95% CI 0.22 to 0.99), of which 74% was explained by SNPs with nonzero effects, but the credible intervals on both estimates were very high (95% CI 0.24 to 0.98). Approximately 27% of the variants had nonzero effects (n = 733,082); however, only 24 were considered to have major effects. Twenty-nine variants were found with sparse effects in at least 1% of the MCMC runs (PIP > 0.01), after controlling for population structure (Fig. 2*B*). Of the 29 variants, 5 are associated with genes related to beak morphology or craniomorphology (Table 1). The strongest effect was found for a SNP on chromosome 3, within the *ppp1cb* gene. The remaining 28 top candidate SNPs were found spread across the genome. Of the other four SNPs associated with bill morphology or craniomorphology, the first two were found on chromosome 2, within the intronic regions of the *Rims2* and *SKAP2* genes. The third was found on chromosome 3, within the intronic region of the *ppp1cb* gene, and the fourth was found on chromosome 7, within the intronic region of the *MGAT5* gene. Of the 29 top candidate

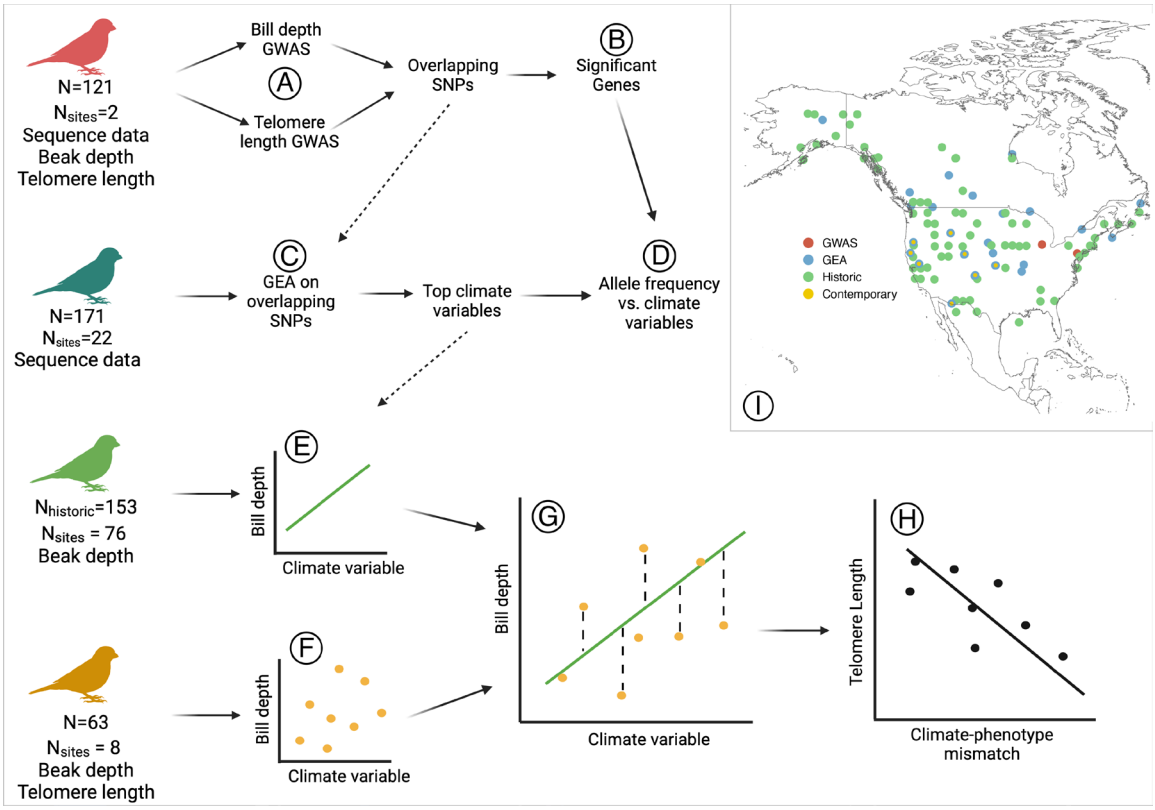

Fig. 1. Workflow for study connecting the genotype, phenotype, and environmental components of local adaptation in the yellow warbler (*S. petechia*), as well effects of maladaptation to climate change. (*A*) We first conduct two separate GWAS on 121 reference individuals from one genetically distinct population to identify a suite of loci related to both bill depth and telomere length. (*B*) Using the results of the GWAS, we find overlapping SNPs with nonzero effects on both bill depth and telomere length. For SNPs with significant effects on at least one of the phenotypes of interest, we then investigate associated genes. (*C*) On the overlapping SNPs from both GWAS, we then run a GEA on 171 individuals from across the yellow warbler range to find environmental variables associated with bill depth and telomere length-associated genomic variation. (*D*) We then aim to validate the significant genes found in (*B*) by looking at the relationship between allele frequencies and values of the top climate variables found in (*C*). (*E*) Using 153 historic yellow warbler samples from across the breeding range, we then analyzed the relationship between bill depth and the top climate variable from (*C*), to find the line of best fit. (*F*) Similarly, we looked at 63 contemporary yellow warbler samples from across the breeding range (samples overlap from *C*) and analyzed the relationship between bill depth and the top climate variable from (*C*). (*G*) We then measured the distance from the line of best fit in (*E*) to each point in (*F*) to quantify climate–phenotype mismatch. (*H*) Finally, we analyze the association between climate–phenotype mismatch and telomere length to find whether distance from the optimal climate–phenotype association is negatively associated with individual quality as we predict. (*I*) Samples span the breeding range of the yellow warbler. The map shows the distribution of the samples for each of associated analysis. The contemporary samples are yellow with a blue border as they are samples also used in the GEA.

SNPs, 17 overlapped with nonzero effect loci identified in the bill-depth GWAS.

Environmental Variables Underlying Bill-Depth Loci Important to Individual Quality. While previous work has used gradient forest to rank which environmental variables are most important to describing general patterns of genetic variation across space (e.g., refs. 52 and 53), here we use gradient forest to identify environmental variables associated specifically with loci underlying bill depth and important to individual quality. To do this, we used the 292,380 overlapping SNPs with nonzero effects between the bill-depth and telomere length GWAS. This use of gradient forest allows us to focus on environmental drivers of local adaptation in a specific phenotype associated with individual quality.

Overall, our GEA analysis found a strong relationship between environmental variables and genomic variation underlying bill-depth loci important to individual quality. Precipitation variables did best at explaining genomic variation, with 6 of the 10 most important predictors in our model representing precipitation measurements (Fig. 3*A*). The top four uncorrelated explanatory variables in our model were BIO18, BIO16, BIO14, and BIO3, which are precipitation of the warmest quarter, precipitation of the wettest quarter, precipitation of the driest month, and isothermality, respectively (Fig. 3*B*). Spatial visualization of these variables indicated that the climate transitions to more precipitation of the warmest quarter with greater precipitation seasonality and less isothermality moving from East to West (Fig. 3*C*).

We used the top-ranking SNPs from each GWAS that also had a nonzero effect in the other phenotype (1 for the bill-depth GWAS and 15 for the telomere length GWAS) to independently validate the association of top candidate SNPs with the top four uncorrelated environmental variables (Fig. 4 and *SI Appendix*, Tables S2–S5). Of the 16 top candidate SNPs, 3 had significant associations between allele frequency and one of the top environmental variables, and two of those were associated with a known gene (*MGAT5* and *RIMS2*; Fig. 4).

Effects of Phenotype–Environment Mismatch on Telomere Length. To test whether the mismatch between bill depth and environment influences telomere length, we used an information-theoretic approach and found that the top ranked model, which also carried a majority of the model weight, included a three-way interaction between phenotype–environment mismatch, climate, and bill depth (Akaike; $w_i = 0.36$; *SI Appendix*, Table S6). To try and disentangle the three-way interaction, we subset the data to only include negative mismatches. As telomere length increases with increasing precipitation and increasing bill depth (*SI Appendix*, Figs. S2 and S3), we expected that in places that are drier and

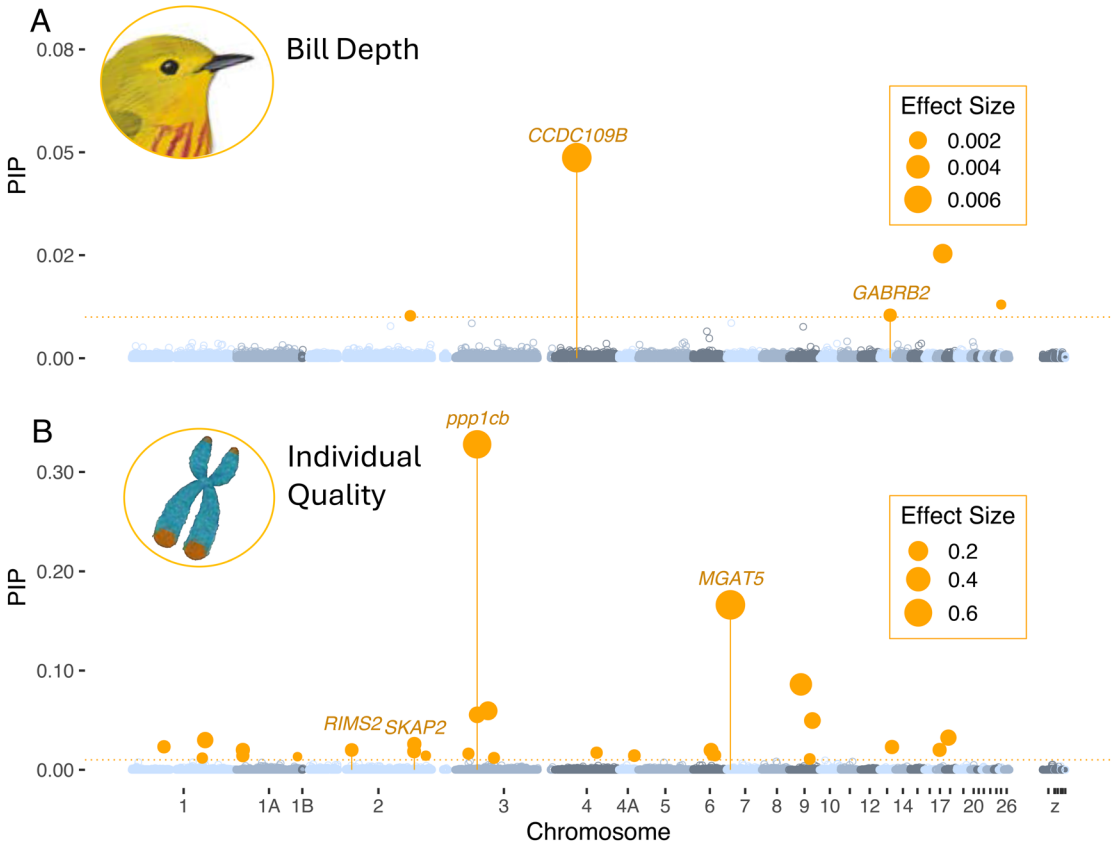

Fig. 2. Manhattan plots of genome-wide association results. (*A*) GWAS results for bill depth with SNPs associated with known genes labeled. (*B*) GWAS results for telomere length (a proxy for individual quality), with genes related to bill morphology and/or craniomorphology labeled. Orange highlights the top candidate SNPs found with sparse effects in at least 1% of the MCMC runs (PIP > 0.01), after controlling for population structure. The size of the top candidate SNPs indicates the effect size. Alternating blue and gray colors indicate chromosomes.

where bills are too shallow (samples with negative mismatches), telomere length will be shortest. Focusing on the relationship between telomere length and phenotype–environment mismatch in the subset data, we found a significant positive association ($P = 0.013$; Fig. 5).

Comparison of Historic and Contemporary Population Structure. We did not find evidence for geographic shifts in population structure over the last century (*SI Appendix*, Fig. S4). The first two principal component axes were highly correlated with geography, an expected result as we designed our SNP panel for geographic assignment. PC1 was most strongly correlated with longitude (F = 1.97e-03, $P < 0.001$), but latitude was also significantly associated with PC1 (F = 8.66e-04, $P < 0.001$). Historical samples did not significantly differ from contemporary samples on PC1 (F = 1.46e-03, $P = 0.464$). PC2 was most strongly correlated with latitude (F = −4.68e-03, $P < 0.001$) but was also correlated with longitude (F = −4.74e-04, $P < 0.001$). Time appeared marginally significant on PC2 (−6.69e-03, $P = 0.065$), but upon further inspection, this pattern was driven by a small number of samples whose low latitudes fell outside the range of contemporary samples. When these samples were removed, we found no effect of time on PC2 loading (F = −4.44e-03, $P = 0.218$). Together, these results show no strong evidence that populations have shifted in their geographic ranges since the 1900s.

Discussion

In this study, we explore the connections between genetic, phenotypic, and environmental drivers of natural selection in the yellow warbler, a species with known linkages between climate change–induced drying and population decline (32, 33). Through GWAS, we identified candidate genes associated with bill morphology and individual quality, several of which have been linked to craniomorphology in other species. Additionally, GEA analyses showed that allele frequency variation within these candidate bill genes was strongly correlated with precipitation across the breeding range, with loci linked to larger bills more prevalent in dryer areas. Comparing current relationships between bill depth and precipitation with preclimate change baselines revealed that contemporary birds with shallower bills in drier areas are experiencing more stress, as indicated by shorter telomeres. Together, these findings indicate that climate change–induced drying may be exerting selective pressure on bill depth, especially in the drier regions of the range. Overall, our results support the hypothesis that bill depth mediates local adaptation to varying precipitation regimes in yellow warblers and that maladaptation resulting from climate change–induced drying may contribute to observed population declines. Although our genomic analyses are inherently correlational due to the observational nature of studies in wild vertebrate populations, we strengthen our inferences by integrating telomere length as a biomarker of individual quality and by demonstrating that phenotype–environment mismatches are associated with increased physiological stress. Together with support from historical data and prior research in this system, these multiple lines of evidence provide a compelling case for local adaptation of bill morphology to precipitation across the breeding range.

In the first part of this study, we used GWAS to investigate the relationships between genotype and phenotype in the yellow

Table 1. Candidate genes identified from results of two GWAS analyses

Phenotype	Chromosome	Marker position (bp)	Gene name	Region	Distance to region	Effect size	PIP	Function	References
Bill depth	4	25876083	*CCDC109B*	Intron 1	0	0.007	0.049	Metabolic processes, feeding efficiency, thermoregulation	(34–37)
Bill depth	18	7991726	Unknown	Regulatory	605	0.002	0.025	Unknown	
Bill depth	27	2283880	Unknown	Intron 2	0	0.001	0.013	Unknown	
Bill depth	13	11897325	*GABRB2*	Intron 5	0	0.001	0.010	Neurotransmission, anxiety-related behavior	(38, 39)
Bill depth	2	115455185	Unknown	Intron 1	0	0.001	0.010	Unknown	
Telomere length	3	31237157	*PPP1CB*	Intron 8	0	0.102	0.055	Head and neck squamous cell carcinoma, morphological adaptation in great tits	(40, 41)
Telomere length	2	52445219	*SKAP2*	Intron 1	0	0.042	0.020	Elevated rates of protein evolution associated with hot- spots of beak shape morphological diversification. Craniofacial development.	(42, 43)
Telomere length	2	119754048	*RIMS2*	Intron 2	0	0.053	0.026	Periodontitis. Head and neck squamous cell carcinoma.	(44, 45)
Telomere length	7	4037108	*MGAT5*	Intron 2	0	0.713	0.166	Craniosyntosis.	(46, 47)
Telomere length	8	334380	*DNM3*	Intron 2	0	0.011	0.006	Hypoxic adaptation in chickens. Crest cushion formation in ducks. Skeletal formation in humans.	(48–51)

In the bill depth GWAS, candidate SNPs were retained if they had sparse effects in at least 1% of the MCMC runs (PIP > 0.01). In the telomere length GWAS, candidate SNPs were retained if they had sparse effects in at least 1% of the MCMC runs and were associated with genes related to beak morphology or craniomorphology. Bslmm was used to estimate effect size and PIP.

warbler, focusing on bill depth and individual quality as the phenotypes (with telomere length as a proxy for individual quality). The combined results from these analyses identified candidate genes associated with cranial morphology, thermoregulation, and bill shape. From these GWAS, we identified significant associations between genetic variation and our phenotypes of interest in 5 genes, 1 of which, *ppp1cb*, is associated with craniomorphology in humans (55, 56). We also identified significant associations with the *SKAP2* gene, which is linked to beak shape and diversification across 72 bird species (42), *Rims2*, which is associated with craniomorphology in birds (57), and *MGAT5* which is associated with craniomorphology in humans (46). Additionally, we identified the *CCDC109B* gene, which is thought to be involved in metabolic processes (e.g., refs. 34 and 35), feeding efficiency (36), and stress-induced thermoregulation (37). Such associations may indirectly influence bill morphology through the efficiency with which a bird can exploit available food sources (e.g., ref. 5) and/or thermoregulate through the surface area of their bill when faced with heat stress (e.g., ref. 16). While further research is needed to confirm the roles these genes play in shaping bill morphology, the fact that our candidate genes were identified in both the bill shape and individual quality (telomere) GWAS adds additional support to the idea that these genes are not only involved in bill morphology but also important to individual quality.

While the first part of our study focused on identifying genes associated with bill shape and individual quality in 121 individuals from two breeding populations, the second part identified environmental variables potentially driving patterns of genetic variation in these genes across 22 populations spanning the breeding range. Our landscape genomic analysis revealed that the top five environmental predictors of genetic variation at bill-linked loci were associated with precipitation, with the top predictor being precipitation of the warmest quarter (BIO18; Fig. 3*A*). If bill shape plays a role in local adaptation as has been suggested by past work in this system (31), we predicted that genetic variation in bill-linked loci would correlate with precipitation across the range. Consistent with this prediction, we found that allele frequency variation was significantly associated with precipitation in 3 of the 17 bill-linked loci identified via GWAS. While past research has shown an association between genome-wide genetic variation and precipitation in yellow warblers (32, 33), here we take this one step further by identifying the association between precipitation and genetic variation in genes specifically linked to bill morphology in the yellow warbler. Specifically, allele frequency in *MGAT5* and *Rims2*, genes known to be associated with craniomorphology, are significantly associated with precipitation of the warmest quarter (BIO18) and isothermality (BIO3), respectively (Fig. 3). The link between precipitation and genetic variation at genes putatively affecting bill morphology lends further support to the idea that changes in precipitation place selective pressure on yellow warblers across time and space.

The link between precipitation and genetic variation in bill-linked loci makes sense considering other research showing that bill morphology plays an important role in heat retention and dissipation as well as water retention in arid environments (e.g., refs. 15, 16, and 58). In small endotherms with high metabolic rates, such as yellow warblers, water loss due to evaporation from the skin and respiratory tract can be very high (59). Beaks, however, are impermeable to evaporative water loss due to their keratin covering and are therefore more effective at dry heat dissipation than other body parts. Hence, larger bills allow for more water savings as more dry heat is dissipated. For example, in song sparrows, a 13.1% increase in bill surface area was estimated to reduce water loss requirements by 7.7% (14). Similarly, in California savannah sparrows, a 7.37% increase in bill size resulted in an estimated 16.2% reduction in water loss (60). Thus, one likely explanation for the link between genetic variation in

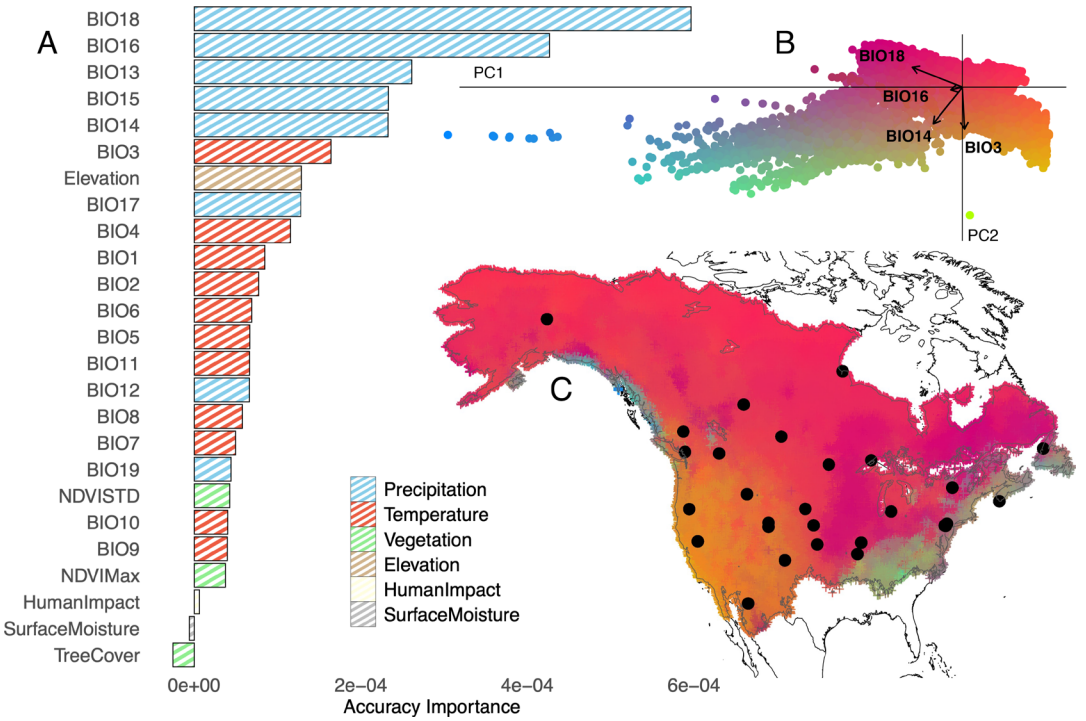

Fig. 3. (*A*) Ranked importance of environmental variables based on gradient forest analysis shows that climate, especially precipitation, strongly explains genomic variation related to bill-depth-linked loci important to individual quality. (*B*) PCA of transformed climate where arrows show the loading of the top 4 uncorrelated climate variables: BIO18 (precipitation of warmest quarter), BIO16 (precipitation of wettest quarter), BIO14 (precipitation of driest month), and BIO3 (isothermality). (*C*) Gradient forest-transformed climate variables show climate adaptation across the breeding range. Points on map reflect sampled locations. Colors are based on the PCA in panel *B*, and show genetic variation is generally associated with drier conditions in the western portion of the yellow warbler breeding range and wetter conditions in the eastern portion of the breeding range.

bill-linked loci and precipitation described herein is that bill depth in the yellow warbler is important for dissipating heat and retaining water in the hottest and driest areas.

Our modern-historical bill size comparison illustrates that climate change–induced disruptions to the relationships between genotype (bill-linked loci), phenotype (bill depth), and the environment (precipitation) may lower individual quality and ultimately result in population declines. Although there are few cases where testing historical associations between morphology and climate are possible, the availability of historical bill measurements of yellow warblers across the breeding range allowed us to compare preclimate change and contemporary associations between bill depth and breeding season precipitation. We predicted that if bill shape is important to local adaptation and climate change has resulted in maladaptation, then deviations from the preclimate change optima would correlate with decreases in individual quality. In keeping with this prediction, our results support the idea that in areas that have gotten drier over time, individuals with shallower bills than expected based on the preclimate change baselines are experiencing significantly more stress (had shorter telomeres) (Fig. 5). As telomeres are suggestive of individual quality, these results support the idea that yellow warblers in areas that have gotten drier may be unable to adapt rapidly enough to keep pace with drying environments, which may increase stress and lower fitness. In addition, our finding that genetic population structure has remained stable over the past century supports the conclusion that

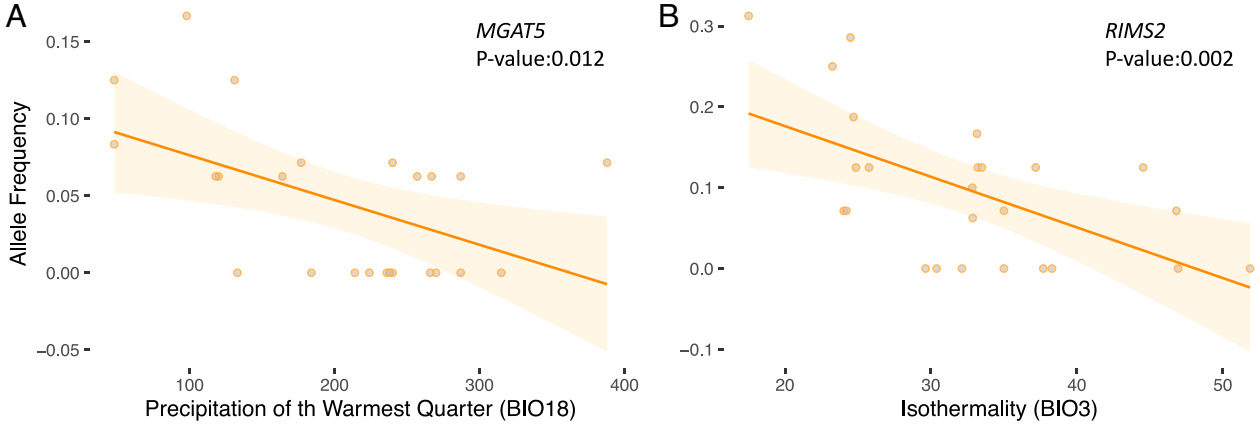

Fig. 4. Associations between top candidate environmental variables and allele frequencies of genes important to bill depth and individual quality. (*A*) Association between allele frequency of MGAT5 gene and precipitation of the warmest quarter (BIO18). (*B*) Association between Rims2 gene and isothermality (BIO3).

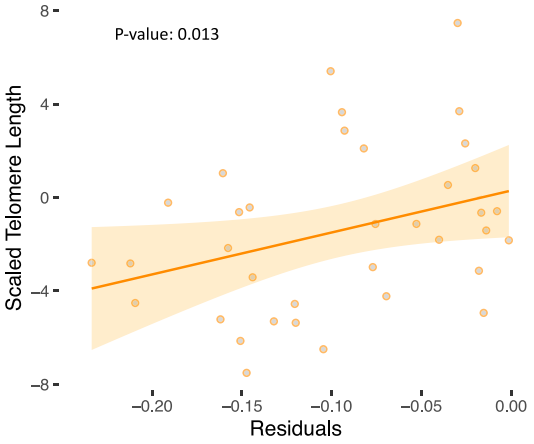

Fig. 5. Subset data (only including negative residuals) looking at association between telomere length and residuals of association between precipitation and bill depth between preclimate and contemporary data. Data from Wiedenfeld (54) were used to determine the preclimate change association between bill depth and breeding-season precipitation, which we then compared to our contemporary data. We then calculated residuals from contemporary data to the line of best fit from the preclimate data, which we used as way to measure the distance from the optimal association between precipitation and bill depth. Data were subset to only include negative residuals, which represent drying areas.

observed maladaptation is not due to shifting population ranges and reflects insufficient evolutionary response to contemporary environmental change. Overall, the impact of climate change–induced drying on individual quality may help explain why an increase in drying is associated with population decline in this species (32, 33). These results lend further support to the idea that larger bills are an adaptation to arid environments through their functioning in heat dissipation and water retention and that climate change–induced increases in aridity may result in maladaptation.

Conclusions

Clear examples of the links between genotype, phenotype, and the environmental drivers of local adaptation are rare in wild populations, and examples of the effects of maladaptation are even rarer. Here, we combine GWAS and GEA analyses to identify genes underlying bill shape in the yellow warbler and examine the role of precipitation in explaining genetic variation within a subset of these bill-linked genes. Using telomere length as a proxy for individual quality, we show that rapid, climate change–induced drying, without corresponding shifts in bill depth, increases stress and likely contributes to observed population declines. Overall, this study represents an important test of the putative links between genotype, phenotype, and the environmental drivers of natural selection. As changes in climate continue to disrupt patterns of local adaptation, this research can serve as a model for assessing the impacts of such disruptions in free-living species where field-based assessments of individual quality are not feasible.

Materials and Methods

Sample Collection and DNA Isolation. We collected samples from 121 yellow warblers from two reference populations in Michigan and Pennsylvania (Fig. 1*I*). At each site, birds were captured using mist-netting, bill depth measurements were taken, and blood samples were collected via brachial venipuncture and preserved in Queens lysis buffer. Further, we collected an additional 171 genetic samples from 22 sites across the yellow warbler breeding range to validate associations between allele frequencies and environmental variables in key loci. From the 171 samples, 63 samples with bill depth measurements from 10 sites across the breeding range were also used to validate the associations between bill depth and environmental variables. DNA from all samples was purified using the Qiagen™ Dneasy Blood and Tissue extraction kit and quantified using the Qubit dsDNA HS Assay kit (Thermo Fisher Scientific).

Whole-Genome Sequencing and Variant Calling. Whole genome sequencing libraries were prepared following modifications of Illumina's Nextera Library Preparation protocol (61) and were sequenced on NovaSeq6000 lanes at Duke University Sequencing and Genomic Technologies with a target sequencing depth of 2× per individual. To process sequence data, we used the workflow management system Snakemake to create a reproducible bioinformatics pipeline (62). We used the program Trimmomatic 0.39 (63) to trim the sequence data to remove Illumina adapter sequences and polyG tails using a sliding window approach (SLIDINGWINDOW:4:20). We then mapped reads to the yellow warbler reference genome (NCBI BioProject PRJNA777222) (64) using BWA 0.7.17 (65) with the bwa mem Snakemake wrapper (v1.23.3/bio/bwa/mem). After mapping, the resulting SAM files were sorted, converted to BAM files, and indexed using Samtools version 1.16 (66). We used MarkDuplicates from Picard (http://broadinstitute.github.io/picard) to mark read duplicates and clipped overlapping reads with the clipOverlap function from bamUtil (67). To reduce sequencing depth variation, we used the downsample function from Picard (http://broadinstitute.github.io/picard) to downsample reads from BAM files with greater than 3× coverage, to 3× coverage. This resulted in an average read depth of 2.7× coverage.

To identify genetic markers from low-coverage WGS data, we used the program HaplotypeCaller in the Genome Analysis Toolkit (GATK version 4.1.6.0) (68) applying a minimum base quality score of 33 and a minimum mapping quality score of 20 to reduce lane effects (69). To parallel the genotype calling process, we generated genomic databases in ~3 Mb intervals across the genome and combined and indexed the genotyped VCF files with BCFtools 1.16 (70). To remove systematic errors, we applied a hard filter to the subsequent VCF file with the following parameters, "QD < 2.0 || FS > 60.0 || MQ < 40.0 || MQRankSum < -12.5 || ReadPosRankSum < -8.0," filtering the indels separately with "QD < 2.0 || FS > 200.0 || ReadPosRankSum < -20.0." We then used BCFtools to keep biallelic sites (-m 2 -M 2) missing in fewer than 20% of the sampled individuals ("F _ MISSING < 0.20"), with minor allele frequency of at least 0.05 (--min-af 0.05, --max-af 0.95), and with a sequencing quality score of at least 30 ("QUAL > 30") (69). This filtering resulted in 2,999,708 variants in 298 individuals with an average of 21% missing data.

Telomere Length Measurement with WGS Data. We measured telomere length from bam files using Telseq v0.0.2 (71), a widely used software developed specifically to calculate telomere length from whole-genome sequence data (e.g., refs. 72–74). Previous comparative analyses found that Telseq is highly correlated with qPCR measurements of telomere content on a panel of cell lines and cell strains, with R-squared values of 0.89 to 0.92 (75). Telseq was also previously validated using 260 leukocyte samples from the TwinsUK cohort, where its estimated mean telomere length was compared to Telomere Restriction Fragment (TRF) estimates (71). Although TelSeq estimates were consistently shorter than TRF estimates, their correlation remained stable across a range of predefined numbers of telomeric repeats (Spearman's Q = 0.6).

Telomere length calculated from Telseq is the cumulative length of telomere repeats normalized based on the GC composition of total reads (48 to 52%), ensuring accurate telomere length estimation by accounting for GC bias. We modified parameters in the Telseq source code to adapt it to the yellow warbler genome, which includes changing the number of chromosomal ends, read length, and total GC content (bp). The parameters TELOMERE_ENDS, READ_LENGTH, and GENOME_LENGTH_AT_TEL_GC were set equal to 62, 100, and 143831148, respectively. We calculated the latter by measuring the total length of 150 base pair windows in the yellow warbler genome with a GC content between 48% and 52%.

GWAS Analysis of Bill Depth Phenotypes and Telomere Length. To investigate the genetic basis of bill depth and telomere length, we first used a GWAS (Fig. 1*A*). Specifically, we applied a Bayesian sparse linear mixed model (BSLMM) (76) implemented in GEMMA (v0.98.3), following an approach similar to Contina et al. (21). This framework integrates features of linear mixed models and Bayesian variable selection regression, allowing detection of both polygenic and oligogenic architectures when the underlying genetic basis is unknown. Because bslmm does not allow the incorporation of covariates into the model, to account for

variation in telomere length due to sex and body size, we regressed telomere length on age, sex, and mass and used the residuals as our telomere length phenotypes. We used similar techniques for bill depth by regressing bill depth on sex and mass and using the residuals as our bill depth phenotypes. To account for population structure, we constructed a genetic relatedness matrix in GEMMA using the 2,999,708 SNPs after quality filtering, imputing missing genotypes with Beagle (v4.1) (77). The BSLMM was run with the kinship matrix for 5 million generations and with a burn-in period of 500,000 iterations. Variants with a posterior inclusion probability (PIP) > 0.01 were considered candidate SNPs. We ordered scaffolds according to the zebra finch (Taeniopygia guttata) genome assembly using Satsuma Synteny (78) and calculated distances between loci. Gene annotations for the zebra finch genome (taeGut3.2.4, GCF_000151805.1) were obtained from Ensembl, and the closest gene to each candidate SNP within 50 kb was identified (Fig. 1*B*) using bedtools closest (v2.30.0) (79).

Environmental Variables Underlying Bill-Depth Loci Important to Individual Quality. To explore environmental correlates of candidate loci associated with bill-depth and individual quality (Fig. 1*C*), we applied gradient forest analysis (R package gradientForest v0.1-34) to allele frequencies from 22 breeding populations at 292,380 candidate SNPs with nonzero effects shared between the GWAS for telomere length and bill depth. Predictor variables included 19 WorldClim climate layers, NDVI and NDVI SD (80), tree cover (81), elevation (https://www.usgs.gov/centers/eros/science/national-land-cover-database), and QuickSCAT-derived surface moisture. Gradient forest models were built with 100 regression trees to rank predictor importance. Spatial predictions across 100,000 random breeding-range points were visualized using PCA on the top three environmental axes, which were then mapped to illustrate adaptive landscape variation.

To validate the association between allele frequencies in bill-depth loci important to individual quality, we calculated the allele frequencies for the top loci that overlapped for bill depth and telomere length for each of our 22 sample locations. We then used linear regression to test the relationships between allele frequency and the four most important uncorrelated climate variables (Fig. 1*D*), applying a Benjamini–Hochberg correction for multiple comparisons.

Effects of Phenotype–Environment Mismatch on Telomere Length. To compare the current and preclimate-change associations between phenotype and environment, we used data from Wiedenfeld (54) which includes morphometric measurements from 153 yellow warblers captured between 1873 and 1987. As a body-size measurement was not included in the historic dataset, we instead used wing-chord as a proxy for body size to calculate body-size corrected bill depth in historic and current samples. Using locations of capture, we extracted historical monthly climate data from Worldclim CRU-TS 4.06 (82) downscaled with WorldClim 2.1 (83) for the breeding months of May, June, and July for each sample between the years of 1901 and 1950, which we then averaged. As bioclim variables are not available for historic time periods, we used an average that captured the most important environmental variable found in the GEA. To ensure consistency and control for confounding variables, we used the same telomere length values, regressed on age, sex, and mass, as those used in the GWAS. We then used the "lm" function in R version 3.5.3 (https://www.R-project.org) to fit linear models to test the association between bill depth and the environment for both our historic and contemporary samples (Fig. 1 *E* and *F*). We then calculated the residuals from the contemporary association to the historical line of best fit (Fig. 1*G*). We used those residuals as a measure of change between the historic and contemporary relationship between bill depth and climate, where a larger residual means a bigger mismatch between bill depth and the environment, relative to what we assume is the preclimate change optimal (*SI Appendix*, Fig. S1).

To test whether the mismatch between bill depth and environment influences telomere length, which we use as a proxy for individual quality, we used an information theoretic approach for model selection and ranking (84) using the package AICcmodavg v2.3-2 in R (Fig. 1*H*). Using the lm function, we constructed a set of linear models with telomere length as our response variable. Our candidate model set included a residual effect model, an environment effect model, and a bill depth effect model. As all our predictor variables have the potential for additive and interactive effects, all combinations of predictor variables were included in the candidate set. A null model was also included.

Comparison of Historic and Contemporary Population Structure. We used population structure analyses to ask whether local populations have shifted their geographic ranges over the last century. We assembled a collection 169 historic samples of yellow warblers sampled on their breeding range. Historic samples were skin or toe pads loaned from museums (*SI Appendix*, Table S1). All samples were extracted using the Qiagen DNeasy Blood and Tissue Kit and genotyped at a set of 96 SNPs, previously identified for geographic assignment (31), using a Fluidigm 96.96 IFC controller. After SNP genotyping, we discarded individuals with poor quality data (<50% of SNPs genotyped). Genotypes from historic samples were combined with previously genotyped contemporary yellow warblers (1990-present) sampled on their breeding range (31). This left us with a final set of 551 samples (129 historical and 422 contemporary).

We performed principal components analysis (PCA) on contemporary samples only to establish the relationship between genetic variation and geography. PCA was performed using the SNPRelate package (85) in R v4.3.2. We then predicted loadings of historical samples using the snpgdsPCASampLoading function. Historical samples were plotted alongside contemporary samples to visualize whether relationships between genetic variation and geography changed over time. We used linear models to test for effects of latitude, longitude, and time (historical v. contemporary) on PC axes.

Data, Materials, and Software Availability. Genome sequences, bird metadata, and code data have been deposited in Dryad (http://datadryad.org/share/ybrYl7ApazkUw2sSxM5LbE2CvWmsvZNehqhRP-r6sAQ) (86).

ACKNOWLEDGMENTS. We thank Eric Anderson for his help and support in the bioinformatic analyses. We also thank the many people who assisted in sample collection, especially Tim Kita, Rich Keith, Brenda Keith, Martin Rodriguez, and the many volunteers from the Institute for Bird Populations, MAPS, and Bird Conservancy of the Rockies for providing or assisting with the collection of samples. We also gratefully acknowledge the following museums for tissue loans of historic samples: Buffalo Society of Natural Sciences, California Academy of Sciences, Carnegie Museum of Natural History, Charles R. Conner Museum, Delaware Museum of Natural History, Denver Museum of Nature & Science, Field Museum of Natural History, University of Kansas Biodiversity Institute, Natural History Museum of Los Angeles County, Museum of Comparative Zoology–Harvard University, Museum of Vertebrate Zoology–UC Berkeley, James R. Slater Museum of Natural History, Royal Ontario Museum, Museum of Wildlife and Fish Biology–UC Davis, University of Michigan Museum of Zoology, and Yale Peabody Museum. This work was made possible by an NSF Graduate Research Fellowship (006784) to M.D.R., an NSF CAREER grant (1942313) to K.C.R., and a National Geographic Grant (62591-443863) to K.C.R.

1. O. Savolainen, M. Lascoux, J. Merilä, Ecological genomics of local adaptation. *Nat. Rev. Genet.* **14**, 807–820 (2013).
2. S. Lamichhaney *et al.*, Evolution of Darwin's finches and their beaks revealed by genome sequencing. *Nature* **518**, 371–375 (2015).
3. L. M. Cook, I. J. Saccheri, The peppered moth and industrial melanism: Evolution of a natural selection case study. *Heredity* **110**, 207–212 (2013).
4. K. Strickland *et al.*, Genome-phenotype-environment associations identify signatures of selection in a panmictic population of threespine stickleback. *Mol. Ecol.* **32**, 1708–1725 (2023).
5. B. R. Grant, P. R. Grant, Evolution of Darwin's finches caused by a rare climatic event. *Proc. R. Soc. Lond. Series B: Biol. Sci.* **251**, 111–117 (1993).
6. S. Lamichhaney *et al.*, A beak size locus in Darwin's finches facilitated character displacement during a drought. *Science* **352**, 470–474 (2016).
7. A. W. Santure, D. Garant, Wild gwas–Association mapping in natural populations. *Mol. Ecol. Resour.* **18**, 729–738 (2018).
8. A. Korte, A. Farlow, The advantages and limitations of trait analysis with GWAS: A review. *Plant Methods* **9**, 1–9 (2013).
9. K. A. Siminovitch, PTPN22 and autoimmune disease. *Nat. Genet.* **36**, 1248–1249 (2004).
10. J. E. Hess, J. S. Zendt, A. R. Matala, S. R. Narum, Genetic basis of adult migration timing in anadromous steelhead discovered through multivariate association testing. *Proc. R. Soc. Lond. B Biol. Sci.* **283**, 20153064 (2016).
11. M. Bonar *et al.*, Genomic correlates for migratory direction in a free-ranging cervid. *Proc. R. Soc. Lond. B Biol. Sci.* **289**, 20221969 (2022).
12. S. L. Lundregan *et al.*, Inferences of genetic architecture of bill morphology in house sparrow using a high-density SNP array point to a polygenic basis. *Mol. Ecol.* **27**, 3498–3514 (2018).

13. M. Bosse *et al.*, Recent natural selection causes adaptive evolution of an avian polygenic trait. *Science* **358**, 365–368 (2017).
14. R. Greenberg, R. Danner, B. Olsen, D. Luther, High summer temperature explains bill size variation in salt marsh sparrows. *Ecography* **35**, 146–152 (2012).
15. M. R. Symonds, G. J. Tattersall, Geographical variation in bill size across bird species provides evidence for Allen's rule. *Am. Nat.* **176**, 188–197 (2010).
16. G. J. Tattersall, B. Arnaout, M. R. Symonds, The evolution of the avian bill as a thermoregulatory organ. *Biol. Rev.* **92**, 1630–1656 (2017).
17. V. L. Sork *et al.*, Putting the landscape into the genomics of trees: Approaches for understanding local adaptation and population responses to changing climate. *Tree Genet. Genomes* **9**, 901–911 (2013).
18. P. Salmón *et al.*, Continent-wide genomic signatures of adaptation to urbanisation in a songbird across Europe. *Nat. Commun.* **12**, 2983 (2021).
19. A. G. Keller *et al.*, Multi-locus genomic signatures of local adaptation to snow across the landscape in California populations of a willow leaf beetle. *Proc. R. Soc. B* **290**, 20230630 (2023).
20. A. R. De La Torre *et al.*, Dissecting the polygenic basis of cold adaptation using genome-wide association of traits and environmental data in Douglas-fir. *Genes* **12**, 110 (2021).
21. A. Contina, C. M. Bossu, D. Allen, M. B. Wunder, K. C. Ruegg, Genetic and ecological drivers of molt in a migratory bird. *Sci. Rep.* **13**, 814 (2023).
22. E. H. Blackburn, J. W. Szostak, The molecular structure of centromeres and telomeres. *Annu. Rev. Biochem.* **53**, 163–194 (1984).
23. E. S. Epel *et al.*, Accelerated telomere shortening in response to life stress. *Proc. Natl. Acad. Sci. U.S.A.* **101**, 17312–17315 (2004).
24. P. Monaghan, Organismal stress, telomeres and life histories. *J. Exp. Biol.* **217**, 57–66 (2014).
25. R. V. Wilbourn *et al.*, The relationship between telomere length and mortality risk in non-model vertebrate systems: A meta-analysis. *Philos. Trans. R. Soc. Lond. B Biol. Sci.* **373**, 20160447 (2018).
26. K. Whittemore, E. Vera, E. Martínez-Nevado, C. Sanpera, M. A. Blasco, Telomere shortening rate predicts species life span. *Proc. Natl. Acad. Sci. U.S.A.* **116**, 15122–15127 (2019).
27. F. Angelier *et al.*, Is telomere length a molecular marker of individual quality? Insights from a long-lived bird. *Funct. Ecol.* **33**, 1076–1087 (2019).
28. M. Le Vaillant *et al.*, Telomere length reflects individual quality in free-living adult king penguins. *Polar Biol.* **38**, 2059–2067 (2015).
29. H. Y. J. Chik *et al.*, Adult telomere length is positively correlated with survival and lifetime reproductive success in a wild passerine. *Mol. Ecol.* **33**, e17455 (2024).
30. H. Froy *et al.*, Heritable variation in telomere length predicts mortality in Soay sheep. *Proc. Natl. Acad. Sci. U.S.A.* **118**, e2020563118 (2021).
31. R. A. Bay *et al.*, Genetic variation reveals individual-level climate tracking across the annual cycle of a migratory bird. *Ecol. Lett.* **24**, 819–828 (2021).
32. R. A. Bay *et al.*, Genomic signals of selection predict climate-driven population declines in a migratory bird. *Science* **359**, 83–86 (2018).
33. M. D. Rodriguez, R. A. Bay, K. C. Ruegg, Telomere length differences indicate climate change-induced stress and population decline in a migratory bird. *Mol. Ecol.*, 10.1111/mec.17642 (2025).
34. G. Gherardi, H. Monticelli, R. Rizzuto, C. Mammucari, The mitochondrial Ca2+ uptake and the fine-tuning of aerobic metabolism. *Front. Physiol.* **11**, 554904 (2020).
35. P. R. Houlihan, "The role of mitochondrial restructuring in neuronal calcium homeostasis and excitotoxicity," Doctoral dissertation, University of Iowa, Iowa City, IA (2013).
36. M. S. Salleh, G. Mazzoni, M. O. Nielsen, P. Løvendahl, H. Kadarmideen, Identification of expression QTLs targeting candidate genes for residual feed intake in dairy cattle using systems genomics. *J. Genet. Genome Res.* **5**, 35 (2018).
37. V. G. Moisiadis, A. Constantinof, A. Kostaki, M. Szyf, S. G. Matthews, Prenatal glucocorticoid exposure modifies endocrine function and behaviour for 3 generations following maternal and paternal transmission. *Sci. Rep.* **7**, 11814 (2017).
38. M. Barki, H. Xue, GABRB2, a key player in neuropsychiatric disorders and beyond. *Gene* **809**, 146021 (2022).
39. A. Fallahsharoudi *et al.*, QTL mapping of stress related gene expression in a cross between domesticated chickens and ancestral red junglefowl. *Mol. Cell. Endocrinol.* **446**, 52–58 (2017).
40. N. Milutin Gašperov *et al.*, DNA methylome distinguishes head and neck cancer from potentially malignant oral lesions and healthy oral mucosa. *Int. J. Mol. Sci.* **21**, 6853 (2020).
41. L. G. Spurgin *et al.*, The great tit HapMap project: A continental-scale analysis of genomic variation in a songbird. *Mol. Ecol. Resour.* **24**, e13969 (2024).
42. L. Yusuf *et al.*, Noncoding regions underpin avian bill shape diversification at macroevolutionary scales. *Genome Res.* **30**, 553–565 (2020).
43. A. Wilderman *et al.*, A distant global control region is essential for normal expression of anterior HOXA genes during mouse and human craniofacial development. *Nat. Commun.* **15**, 136 (2024).
44. H. Kim *et al.*, Differential DNA methylation and mRNA transcription in gingival tissues in periodontal health and disease. *J. Clin. Periodontol.* **48**, 1152–1164 (2021).
45. N. Stransky *et al.*, The mutational landscape of head and neck squamous cell carcinoma. *Science* **333**, 1157–1160 (2011).
46. A. T. Timberlake *et al.*, De novo variants implicate chromatin modification, transcriptional regulation, and retinoic acid signaling in syndromic craniosynostosis. *Am. J. Hum. Genet.* **110**, 846–862 (2023).
47. A. Dudakovic, H. K. Nam, A. vanWijnen, N. E. Hatch, Modifiers and mediators of craniosynostosis severity revealed by differential gene expression. bioRxiv [Preprint] (2020). https://doi.org/10.1101/2020.01.28.923508.
48. Y. Hu, J. Su, L. Cheng, D. Lan, D. Li, Pectoral muscle transcriptome analyses reveal high-altitude adaptations in Tibetan chickens. *Anim. Biol.* **70**, 385–400 (2020).
49. G. Chang *et al.*, The first crested duck genome reveals clues to genetic compensation and crest cushion formation. *Genom. Proteom. Bioinform.* **21**, 483–500 (2023).
50. T. Ashraf *et al.*, Two further patients with the 1q24 deletion syndrome expand the phenotype: A possible role for the miR199–214 cluster in the skeletal features of the condition. *Am. J. Med. Genet. A* **167**, 3153–3160 (2015).
51. H. Lefroy, O. Fox, M. K. Javaid, T. Makaya, D. J. Shears, 1q24 deletion syndrome. Two cases and new insights into genotype–phenotype correlations. *Am. J. Med. Genet. A* **176**, 2004–2008 (2018).
52. A. Tigano *et al.*, Genomic vulnerability of a freshwater salmonid under climate change. *Evol. Appl.* **17**, e13602 (2024).
53. K. Ruegg *et al.*, Ecological genomics predicts climate vulnerability in an endangered southwestern songbird. *Ecol. Lett.* **21**, 1085–1096 (2018).
54. D. A. Wiedenfeld, Geographical morphology of male yellow warblers. *Condor* **93**, 712–723 (1991).
55. C. H. Lin *et al.*, Epileptic spasms in PPP1CB–associated Noonan-like syndrome: A case report with clinical and therapeutic implications. *BMC Neurol.* **18**, 1–6 (2018).
56. P. Vaneynde, I. Verbinnen, V. Janssens, The role of serine/threonine phosphatases in human development: Evidence from congenital disorders. *Front. Cell Dev. Biol.* **10**, 1030119 (2022).
57. E. Abernathy, "The genomic basis of population and adaptive divergence in buteo sister species across multiple evolutionary and geographic scales," Doctoral dissertation, University of California Davis, Davis, CO (2021).
58. R. Greenberg, V. Cadena, R. M. Danner, G. Tattersall, Heat loss may explain bill size differences between birds occupying different habitats. *PLoS One* **7**, e40933 (2012).
59. J. R. Speakman, E. Król, The heat dissipation limit theory and evolution of life histories in endotherms–Time to dispose of the disposable soma theory? *Integr. Comp. Biol.* **50**, 793–807 (2010).
60. P. M. Benham, R. C. Bowie, The influence of spatially heterogeneous anthropogenic change on bill size evolution in a coastal songbird. *Evol. Appl.* **14**, 607–624 (2021).
61. T. M. Schweizer, M. G. DeSaix, Cost-effective library preparation for whole genome sequencing with feather DNA. *Conserv. Genet. Resour.* **15**, 21–28 (2023).
62. J. Köster, S. Rahmann, Snakemake–A scalable bioinformatics workflow engine. *Bioinformatics* **28**, 2520–2522 (2012).
63. A. M. Bolger, M. Lohse, B. Usadel, Trimmomatic: A flexible trimmer for Illumina sequence data. *Bioinformatics* **30**, 2114–2120 (2014).
64. W. L. Tsai *et al.*, A highly contiguous genome assembly for the Yellow Warbler (Setophaga petechia). *J. Hered.* **115**, 317–325 (2024).
65. H. Li, R. Durbin, Fast and accurate short read alignment with Burrows-Wheeler transform. *Bioinformatics* **25**, 1754–1760 (2009).
66. H. Li *et al.*; Genome Project Data Processing Subgroup, The sequence alignment/map format and SAMtools. *Bioinformatics* **25**, 2078–2079 (2009).
67. G. Jun, M. K. Wing, G. R. Abecasis, H. M. Kang, An efficient and scalable analysis framework for variant extraction and refinement from population-scale DNA sequence data. *Genome Res.* **25**, 918–925 (2015).
68. G. A. Van der Auwera *et al.*, From fastq data to high-confidence variant calls: The genome analysis toolkit best practices pipeline. *Curr. Protoc. Bioinformatics* **43**, 11.10.1–11.10.33 (2013).
69. R. N. Lou, N. O. Therkildsen, Batch effects in population genomic studies with low-coverage whole genome sequencing data: Causes, detection and mitigation. *Mol. Ecol. Resour.* **22**, 1678–1692 (2022).
70. P. Danecek *et al.*, Twelve years of SAMtools and BCFtools. *Gigascience* **10**, giab008 (2021).
71. Z. Ding *et al.*, Estimating telomere length from whole genome sequence data. *Nucleic Acids Res.* **42**, e75 (2014).
72. M. A. Taub *et al.*, Genetic determinants of telomere length from 109, 122 ancestrally diverse whole-genome sequences in TOPMed. *Cell Genomics* **2**, 100084 (2022).
73. A. V. Igoshin, N. S. Yudin, G. A. Romashov, D. M. Larkin, A multibreed genome-wide association study for cattle leukocyte telomere length. *Genes* **14**, 1596 (2023).
74. M. Zavala-Paez, J. Holliday, J. A. Hamilton, Leveraging whole-genome sequencing to estimate telomere length in plants. *Mol. Ecol. Resour.* **24**, e13899 (2024).
75. M. Lee *et al.*, Comparative analysis of whole genome sequencing-based telomere length measurement techniques. *Methods* **114**, 4–15 (2017).
76. X. Zhou, P. Carbonetto, M. Stephens, Polygenic modeling with Bayesian sparse linear mixed models. *PLoS Genet.* **9**, e1003264 (2013).
77. B. L. Browning, S. R. Browning, Genotype imputation with millions of reference samples. *Am. J. Hum. Genet.* **98**, 116–126 (2016).
78. M. G. Grabherr *et al.*, Genome-wide synteny through highly sensitive sequence alignment: Satsuma. *Bioinformatics* **26**, 1145–1151 (2010).
79. A. R. Quinlan, BEDTools: The swiss-army tool for genome feature analysis. *Curr. Protoc. Bioinformatics* **47**, 11–12 (2014).
80. M. L. Carroll, C. M. DiMiceli, R. A. Sohlberg, J. R. G. Townshend, *250m MODIS Normalized Difference Vegetation Index* (University of Maryland, College Park, MD, 2004).
81. J. O. Sexton *et al.*, Global, 30-m resolution continuous fields of tree cover: Landsat-based rescaling of MODIS vegetation continuous fields with lidar-based estimates of error. *Int. J. Digit. Earth* **6**, 427–448 (2013).
82. I. Harris, T. J. Osborn, P. D. Jones, D. H. Lister, Version 4 of the CRU TS monthly high-resolution gridded multivariate climate dataset. *Sci. Data* **7**, 109 (2020).
83. S. E. Fick, R. J. Hijmans, WorldClim 2: New 1km spatial resolution climate surfaces for global land areas. *Int. J. Climatol.* **37**, 4302–4315 (2017).
84. K. P. Burnham, D. R. Anderson, *Model Selection and Multimodel Inference: A Practical Information-Theoretic Approach* (Springer, New York, ed. 2, 2002).
85. X. Zheng *et al.*, A high-performance computing toolset for relatedness and principal component analysis of SNP data. *Bioinformatics* **28**, 3326–3328 (2012).
86. M. Rodriguez, Data from "Genetic, phenotypic, and environmental drivers of local adaptation and climate change–induced maladaptation in yellow warblers. Dryad. http://datadryad.org/share/ybrYl7ApazkUw2sSxM5LbE2CvWmsvZNehqhRP-r6sAQ. Deposited 23 May 2025.